



**Table I.** Design of Electrospun Experiment (Variable and Level)

Variable	Variable description	Level ( $k_1$ - $k_4$ )
$j_1$	Polymer concentration (%)	24, 26, 28, 30
$j_2$	Applied voltage (kV)	15, 18, 20, 22
$j_3$	Collector distance (cm)	10, 15, 20, 25
$j_4$	Solvent ratio (DCM/DMF)	9/1, 7/3, 5/5, 3/7

influences on the morphology, diameter, and uniformity of the electrospun polymer fibers.<sup>20</sup> Therefore, in order to obtain the defined uniform fibrous scaffolds with perfect morphology and small diameter, it is necessary to study the controlled parameters. Range analysis is a common method, which can help us analyze the experimental data intuitively. However, to the best of our knowledge, the attempt of using this method to find out the optimum conditions for electrospinning PCLA fibers has never been reported. In addition, the influence of the parameters has been arranged in order. So, the contribution of these parameters on fibers' morphology and diameter can be seen clearly.

In this study, PCLA fibers were electrospun from the home-made copolymer. The optimum electrospinning process parameters such as solvent ratio, applied voltage, collector distance, and solution concentration were found out. The effect of these parameters was arranged in order and each parameter's single effect on fiber diameter, uniformity, and morphology was studied.

## EXPERIMENTAL

### Materials

Poly(lactic acid (PLA,  $M_w = 5000$  g/mol) was provided by Changchun Institute of Applied Chemistry (Jilin, China). Poly( $\epsilon$ -caprolactone) di-OH (PCL-diOH, PCL230) was obtained from Daicel Chemical Industries, Japan. Hexamethylene diisocyanate (HDI) was purchased from Aladdin Reagent. 1,4-

Dioxane was obtained from Guangfu Fine Chemical Research Institute (Tianjin, China). Chloroform (Tianjin Tiantai Fine Chemical Co., China) was used to clean the synthesized copolymer. Methanol was produced by Beijing Chemical Works, China. Dichloromethane (DCM, Tianjin Tiantai Fine Chemical Co., China), and *N,N*-Dimethylformamide (DMF, Xilong Chemical Co., China) were used as solvents directly.

### Preparation of (ABA)<sub>n</sub> Type of PCLA Copolymer

1.5 g PCL-diOH and 3.5 g PLA were dissolved in 30 mL 1,4-dioxane and the temperature was increased to 60°C. Then HDI was slowly added into the solution in a molar ratio of OH : NCO = 1.0 : 3.0. The solution was bubbled with nitrogen gas for 30 min to remove the soluble oxygen. The reaction was conducted at 82°C for 6 h under mechanical stirring. After that, when the temperature cooled down, the solution was precipitated into methanol and stayed for 12 h. Then, the precipitate was filtered under vacuum, till the product became constant. In order to purify the product, it was then dissolved in chloroform and precipitated in methanol again. The filtered polymer was followed by vacuum drying till the solvent evaporated thoroughly.

### Electrospinning Process Design

In order to minimize the number of experiments, an orthogonal experiment was designed. It was not only helpful to measure the influence of four major processing parameters on fibers' average diameter, but also conducive to optimize the conditions for electrospinning PCLA fibers. The total four parameters consisted of solvent ratio, polymer concentration, applied voltage, and collector distance. The variable experiment was shown in Table I.

The selected experimental design was four-level factorial design and provided 16 experiment settings for four variables. A specific experimental design was listed in Table II. The values in the brackets were coded values of the factors.

**Table II.** Scheme of the Experiments

Experiment No.	Polymer concentration $j_1$ (%)	Applied voltage $j_2$ (kV)	Collector distance $j_3$ (cm)	Solvent ratio $j_4$ (DCM/DMF)
1	(1) 24	(1) 15	(1) 10	(1) 9/1
2	(1) 24	(2) 18	(2) 15	(2) 7/3
3	(1) 24	(3) 20	(3) 20	(3) 5/5
4	(1) 24	(4) 22	(4) 25	(4) 3/7
5	(2) 26	(1) 15	(2) 15	(3) 5/5
6	(2) 26	(2) 18	(1) 10	(4) 3/7
7	(2) 26	(3) 20	(4) 25	(1) 9/1
8	(2) 26	(4) 22	(3) 20	(2) 7/3
9	(3) 28	(1) 15	(3) 20	(4) 3/7
10	(3) 28	(2) 18	(4) 25	(3) 5/5
11	(3) 28	(3) 20	(1) 10	(2) 7/3
12	(3) 28	(4) 22	(2) 15	(1) 9/1
13	(4) 30	(1) 15	(4) 25	(2) 7/3
14	(4) 30	(2) 18	(3) 20	(1) 9/1
15	(4) 30	(3) 20	(2) 15	(4) 3/7
16	(4) 30	(4) 22	(1) 10	(3) 5/5

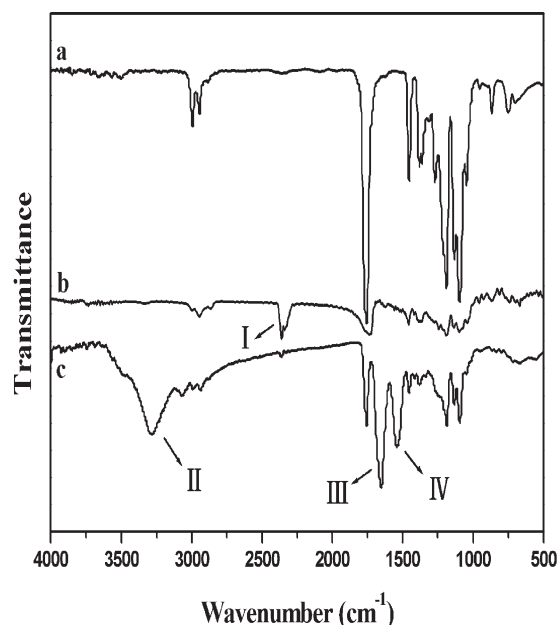


**Figure 1.** The FT-IR spectra of (a) PLA/PCL-diOH blends; and the PCL-diOH/PLA chain linked with HDI for (b) 2 h; (c) 6 h.

After confirmed the optimum conditions, we investigated the single effect of the four variables on fibers' diameter and morphology as well. First, the solvent volume ratio (DCM/DMF) was varied with concentration set at 28 wt %, distance set at 20 cm and applied voltage set at 20 kV. Second, applied voltage was varied with concentration set at 28 wt %, solvent ratio set at 5/5 and distance set at 20 cm. Third, working distance was varied with concentration set at 28 wt %, applied voltage set at 20 kV and solvent ratio set at 5/5. Finally, polymer solution concentration was varied with solvent ratio set at 5/5, distance set at 20 cm and applied voltage set at 20 kV.

#### Characterization

Fourier transform-Infrared radiation (FT-IR) spectrometer (SHIMDZU, 1.50SU1, Japan) was used to identify the vibration in functional groups presented in the samples. The spectra were obtained with 20 scans per sample ranging from 4000 to 400  $\text{cm}^{-1}$ .  $^1\text{H-NMR}$  spectra were recorded using a BRUKER AVANCE 500  $^1\text{H-NMR}$  spectrophotometer and were obtained at room temperature from 15% (w/v)  $\text{CDCl}_3$  solutions. The molecular weight of the sample was determined by gel permeation chromatography (GPC, PL-GPC 220, Polymer Laboratories.).

The fibers were sputter coated with gold using ETD-2000 auto sputter coater (Elaborate Technology Development Co., China) with a current of 4 mA for 2 min. The morphology and dimensions of the fibers were analyzed by scanning electron microscope (SEM; SHIMDZU SSX-550, Japan). Based on the SEM images, the diameter of fibers was analyzed using image visualization software Image J (about 100 measurements per field).

## RESULTS AND DISCUSSION

### Structure Inspections of the Copolymer

**FT-IR Spectra.** Figure 1 shows the FT-IR spectra of PLA and PCL-diOH blends and the PCL-diOH /PLA chain linked with

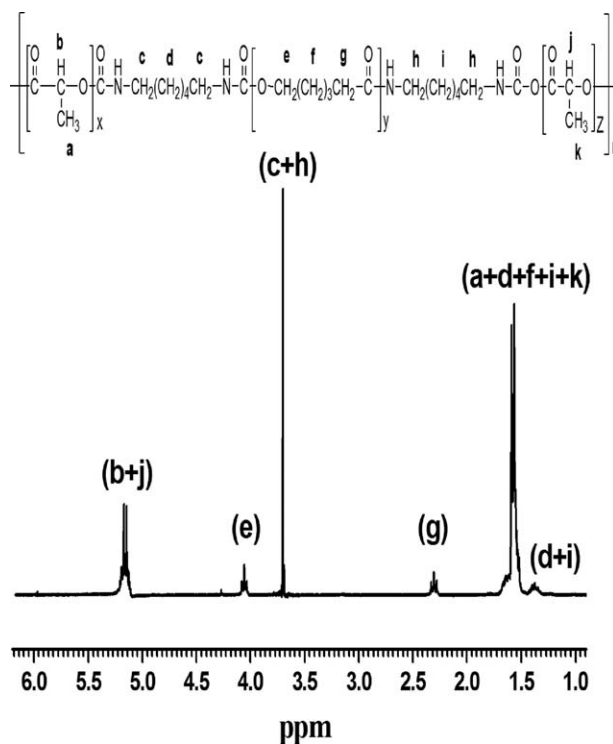


**Figure 2.** The  $^1\text{H-NMR}$  spectroscopy of PCLA multiblock copolymer.

HDI for different times. It was obvious that new peaks occurred after the chain extension reaction. The peak at  $1664\text{ cm}^{-1}$  (III) was the amide bond formed by the reaction between  $-\text{COOH}$  and  $-\text{NCO}$  groups. Another amide bond of urethane appeared at  $1539\text{ cm}^{-1}$  (IV). The appearance of the peak at  $3287\text{ cm}^{-1}$  (II) proved that  $\text{N-H}$  was formed. Comparing Figure 1(a) with (b), it can be observed that the peak at  $2270\text{ cm}^{-1}$  (I) occurred in two hours after added HDI. It corresponded to the  $-\text{NCO}$  groups.<sup>17</sup> However, when the reaction performed for 6 h [Figure 1(c)], peak I disappeared. This demonstrated that HDI had reacted completely.

**$^1\text{H-NMR}$  Spectroscopy.** The  $^1\text{H-NMR}$  spectroscopy of PCLA was shown in Figure 2. The signals appeared at  $^1\text{H NMR}$  (300 MHz,  $\text{CDCl}_3$ ,  $\delta$ ): 1.37 (*m*,  $J=2.3$  Hz, 2H,  $\text{NHCH}_2\text{CH}_2\text{CH}_2\text{CH}_2\text{CH}_2$ ), 2.3 (*t*,  $J=0.8$  Hz, 2H,  $\text{CH}_2\text{CO}$ , PCL), 3.68 (*d*,  $J=2.2$  Hz, 8H,  $\text{NHCH}_2$ ), 4.05 (*t*,  $J=2.5$  Hz, 2H,  $\text{CH}_2\text{O}$ , PCL), and 5.16 (*d*,  $J=3.6$  Hz, 2H, CH, PLA). The peak at 1.5–1.56 belonged to  $\text{NHCH}_2\text{-CH}_2\text{CH}_2\text{CH}_2\text{CH}_2\text{-CH}_2\text{NH}$ , which was overlapped by the peak of methylene protons for PCL-diOH and methyl protons for PLA. All the peaks indicated that PLA and PCL-diOH were successfully connected by HDI.

**GPC Data.** The molecular weight of PLA, PCL-diOH, and the synthetic sample was shown in Table III. From Table III, it can

**Table III.** GPC Data of Different Samples

Sample	$M_w$	$M_n$
PLA	5336	4873
PCL-diOH	3000	-
PLA-PCL-diOH	1,11,213	62,069

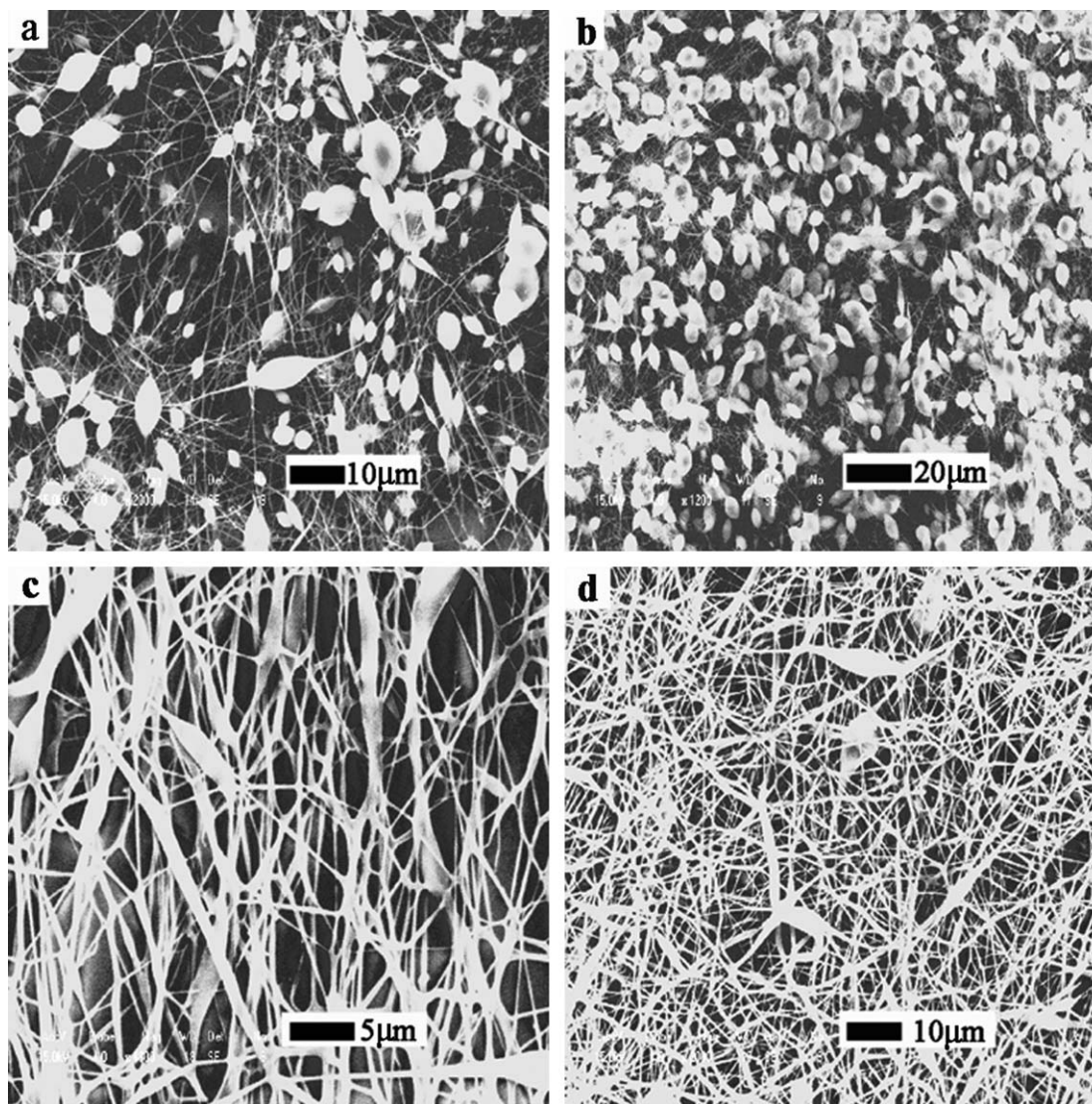


Figure 3. SEM images of experiment (a) 4, (b) 6, (c) 9, and (d) 15 designed in Table II. (The volume ratio of DCM to DMF is 3/7.)

Table IV. Mean Diameter and Standard Deviation of Each Experiment Designed in Table II

Experiment No.	$y_i$ Mean diameter $\pm$ standard deviation ( $\mu\text{m}$ )	Experiment no.	$y_i$ Mean diameter $\pm$ standard deviation ( $\mu\text{m}$ )
1	$3.240 \pm 2.078$	9	-
2	$0.955 \pm 0.324$	10	$0.778 \pm 0.316$
3	$0.568 \pm 0.240$	11	$1.054 \pm 0.309$
4	-	12	$1.544 \pm 0.460$
5	$1.100 \pm 0.559$	13	$1.395 \pm 0.330$
6	-	14	$1.332 \pm 0.430$
7	$1.627 \pm 0.754$	15	-
8	$1.393 \pm 0.285$	16	$0.982 \pm 0.227$

be seen that the molecular weight of PLA and PCL-diOH was 5336 and 3000 respectively, whereas the prepared polymer was 111,213. The results further demonstrated that PLA and PCL-diOH had polymerized successfully.

**The Optimum Conditions for Electrospinning.** The morphology of the PCLA fibers fabricated at a solvent ratio of 3/7 (DCM/DMF) was shown in Figure 3. It can be discovered that lots of beads appeared on the fibers and some fibers adhered together seriously at the ratio. Diameter statistics were influenced significantly by the morphology, so the level of 3/7 was ignored. Mean diameters of the fibers electrospun at other ratios were measured by Image J software and the results were listed in Table IV (their morphologies were provided in Supporting Information).  $y_i$  was experiment index, in this article, it was the average diameter.

After calculation, Table V was obtained. In the table,  $y_{j,k}$  represented the corresponding experiment index of variable  $j$ , level  $k$ .

**Table V.** The Statistic Results of Each Variable and Level

	Diameter $\pm$ standard deviation ( $\mu\text{m}$ )			
	Polymer concentration $j_1$ (%)	Applied voltage $j_2$ (kV)	Collector distance $j_3$ (cm)	Solvent ratio $j_4$ (DCM/DMF)
$Y_{j,1}$	$4.763 \pm 2.642$	$5.735 \pm 2.967$	$5.726 \pm 2.614$	$7.743 \pm 3.722$
$Y_{j,2}$	$4.120 \pm 1.598$	$3.065 \pm 1.070$	$3.599 \pm 1.343$	$5.247 \pm 1.248$
$Y_{j,3}$	$3.376 \pm 1.085$	$3.699 \pm 1.303$	$3.293 \pm 0.955$	$3.428 \pm 1.342$
$Y_{j,4}$	$3.709 \pm 0.987$	$3.919 \pm 0.972$	$3.800 \pm 1.400$	-
$\bar{Y}_{j,1}$	$1.5877 \pm 0.8807$	$1.9117 \pm 0.9890$	$1.9087 \pm 0.8713$	$1.9358 \pm 0.9305$
$\bar{Y}_{j,2}$	$1.3733 \pm 0.5327$	$1.0217 \pm 0.3567$	$1.1997 \pm 0.4477$	$1.3118 \pm 0.3120$
$\bar{Y}_{j,3}$	$1.1253 \pm 0.3617$	$1.2330 \pm 0.4343$	$1.0977 \pm 0.3183$	$0.8570 \pm 0.3355$
$\bar{Y}_{j,4}$	$1.2363 \pm 0.3290$	$1.3063 \pm 0.3240$	$1.2667 \pm 0.4667$	-
$R_j$	$0.4624 \pm 0.5190$	$0.8900 \pm 0.6323$	$0.8110 \pm 0.5530$	$1.0788 \pm 0.5950$
Optimum level	$j_{1,3}$	$j_{2,2}$	$j_{3,3}$	$j_{4,3}$
Effect	$j_4 > j_2 > j_3 > j_1$			
optimum combination	$j_{1,3}, j_{2,2}, j_{3,3}, j_{4,3}$			

For an example,  $y_{3,2}$  means the collector distance is 15 cm (known from Table I). Then from Table II, it can be found that the experiment number 2, 5, 12, and 15 correspond to this distance. So the value of  $y_{3,2}$  can be calculated as follows:

$$y_{3,2} = y_2 + y_5 + y_{12} + y_{15} \quad (1)$$

$\bar{y}_{j,k}$  was the average number of  $y_{j,k}$  (here, because  $y_{15}$  was ignored,  $\bar{y}_{3,2} = y_{3,2}/3$ ). The optimum experiment condition of variable  $j$  could be determined by  $\bar{y}_{j,k}$ . Combining the optimum condition of each variable together, the ideal conditions of entire experiment could be obtained.  $R_j$  was the range of variable  $j$ . The calculate formula was written as

$$R_j = \max [\bar{y}_{j,1}, \bar{y}_{j,2}, \dots] - \min [\bar{y}_{j,1}, \bar{y}_{j,2}, \dots] \quad (2)$$

From Table V, it was obvious that  $\bar{y}_{1,3}$  ( $1.1253 \pm 0.3617 \mu\text{m}$ ),  $\bar{y}_{2,2}$  ( $1.0217 \pm 0.3567 \mu\text{m}$ ),  $\bar{y}_{3,3}$  ( $1.0977 \pm 0.3183 \mu\text{m}$ ) and  $\bar{y}_{4,3}$  ( $0.8570 \pm 0.3355 \mu\text{m}$ ) was, respectively the smallest number in its own variable. The four values corresponded to a concentration of

28 wt %, an applied voltage of 18 kV, a collector distance of 20 cm and a solvent ratio of 5/5. Thus, the optimum conditions for preparing the PCLA fibers were obtained. It also could be discovered that  $R_4 > R_2 > R_3 > R_1$ . This demonstrated that the effect of solvent ratio on diameter was the most significant and the next was applied voltage, collector distance, and solution concentration successively. Fibers fabricated under the optimum condition were shown in Figure 4. It was obvious that the morphology was perfect, and the diameters were uniform. The mean diameter was  $0.77 \mu\text{m}$  and the uniformity was above 80%. What's more, from Figure 4(b), the percentage of diameter in the range of  $0.6\text{--}1.0 \mu\text{m}$  was over 90%. This indicated that most of the fiber diameters were less than  $1.0 \mu\text{m}$ .

#### Single Effect of the Four Variables

**Solvent.** In Figure 5(a–c), when the content of DMF was below 20%, the diameter was large ( $4.885$ ,  $1.93$ , and  $1.86 \mu\text{m}$ ) and the fibers were non-uniform [Figure 5(h)]. With an increase of

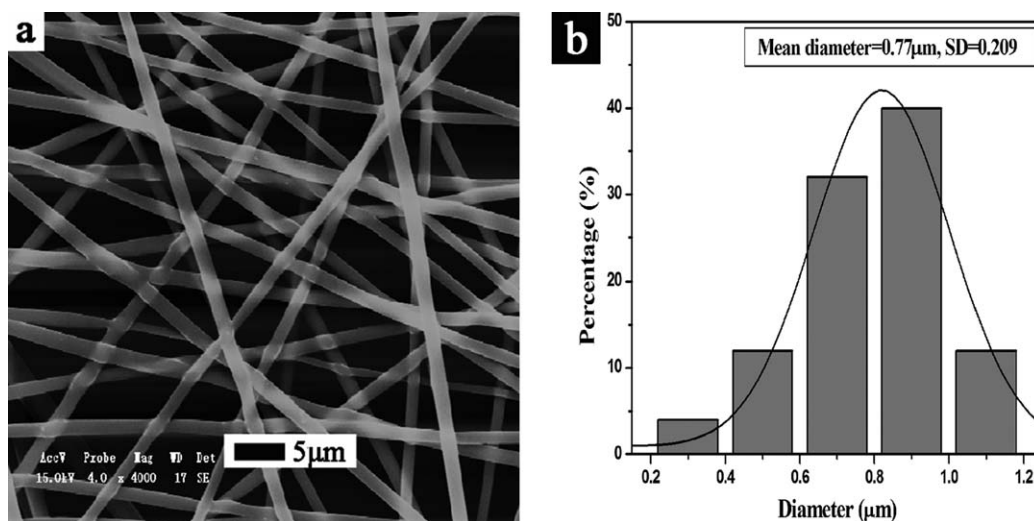


**Figure 4.** Fibers spinning at the optimum conditions: (a) morphology and (b) diameter distribution.

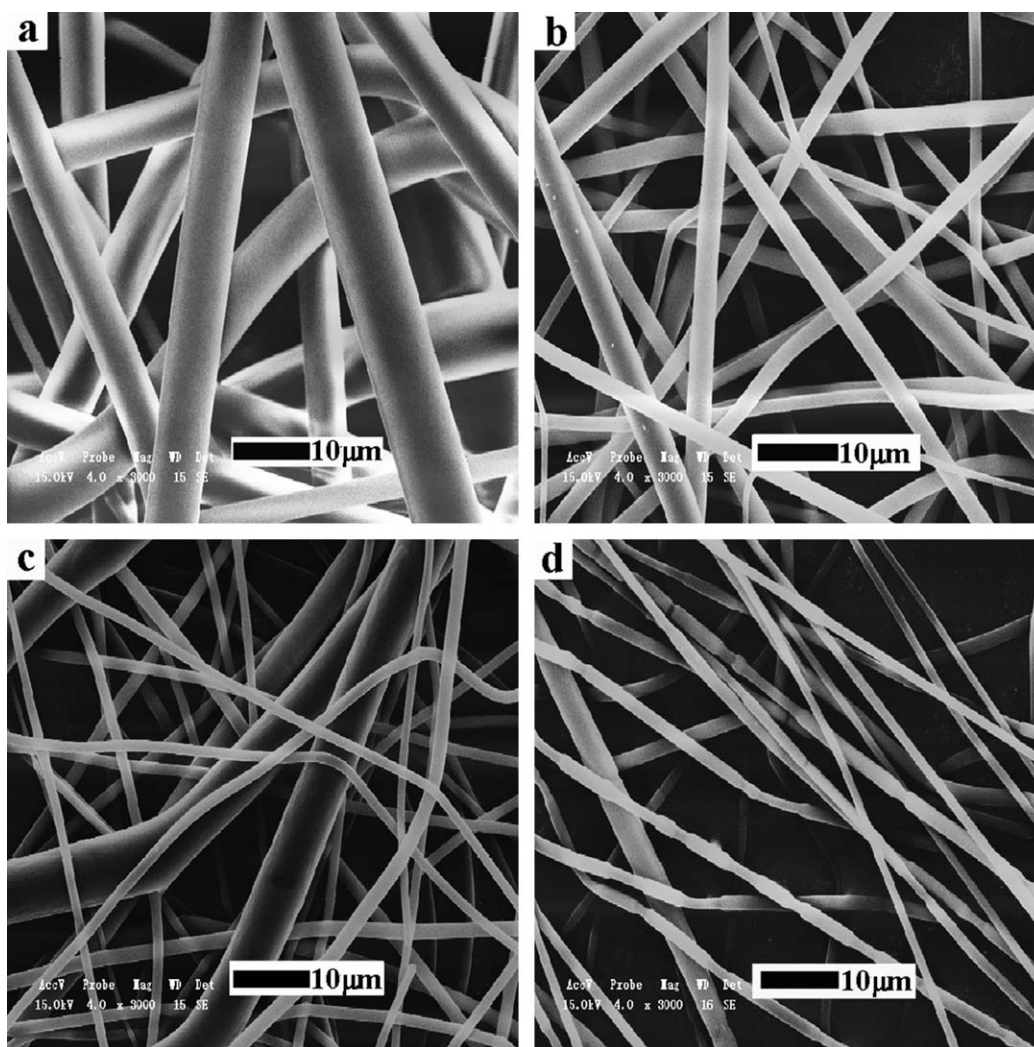


**Figure 5.** SEM images of PCL fibers, the ratios of DCM to DMF are (a) 10/0, (b) 9/1, (c) 8/2, (d) 7/3, (e) 6/4, (f) 5/5, (g) 4/6; (h) is the diameter statistic result of the above images.

DMF content, the fibers tended to be uniform and slim [Figure 5(d–f)]. In the process of electrospinning, solvent with high volatility evaporated speedily. The jet had solidified in the stretch procedure so that it cannot be stretched into slenderer fibers. In contrast, solvent with low volatility could provide enough time for stretching, so fibers with smaller diameter can be obtained. The uniformity was determined by the conductivity of the solvent.<sup>21</sup> Solvent with high conductivity was inclined to fabricate fibers with high uniformity. According to the material information, the conductivities of DCM and DMF are  $4.3 \times 10^{-3} \mu\text{S/cm}$  and  $6 \mu\text{S/cm}$ , respectively. When the content of DMF increased, the solvent conductivity was increased. This explained why the uniformity of fibers was increased with the increasing content of DMF. However, the content of DMF cannot increase freely. When the proportion of DMF was 60%, few fibers stuck together with each other [Figure 5(g)]. This was due to the exceeded low volatility of the solvent. Figure 5 depicts that the effect of solvent on diameter and uniformity was significant. When the content of DMF was proper, diameter of the fibers can be decreased dramatically and the uniformity can be

increased appropriately. It is obvious that mixed solvent is a key factor for obtaining slim and uniform fibers.

**Voltage.** Figure 6 shows the morphology of fibers fabricated under different voltages. When the voltage was 17 kV [Figure 6(a)], fibers stuck together due to weak electrostatic force. The diameter was  $1.447 \mu\text{m}$  and the uniformity was undesirable [Figure 6(b)]. The fibers fabricated at 20 kV were smoothest [Figure 6(b)] and slimmest (the mean diameter was  $1.016 \mu\text{m}$ ). The decrease of fiber diameter was caused by the increase of electrostatic force,<sup>22</sup> which can stretch the jet sufficiently. As voltage further increased, the fibers stuck together again [Figure 6(d,e)] and the diameter was increased [Figure 6(f)]. This phenomenon had been reported by Demir et al.<sup>23</sup> On one hand, driven by high electrostatic force, a large amount of solution aggregated at the tip. It then transformed into a jet with a large diameter. On the other hand, the high electrostatic force shortened the time for stretching. Thus, by the effect of the two functions, the fibers cannot be stretched sufficiently and separate from each other thoroughly before arriving at the collector.

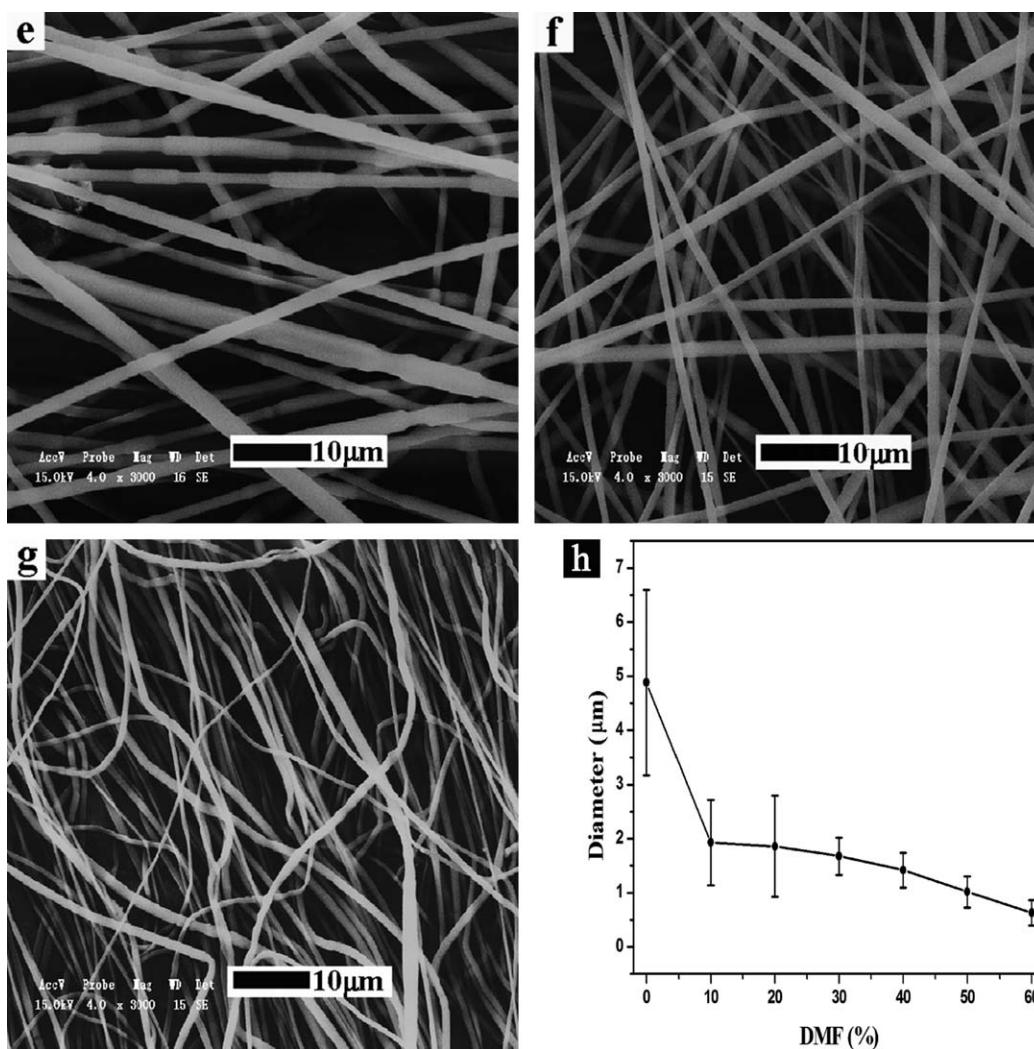


Figure 5. (Continued)

As a result, sticky fibers were obtained. When the voltage was 22, 25, or 28 kV, the range of the error bar was extremely broad. It indicated that the fibers were very non-uniform. This was caused by the adhesion of fibers. In a word, the effect of voltage on fibers' morphology and uniformity was more significant than that on fibers' diameter.

**Distance.** From Figure 7, it can be observed that when the distance was 10 or 15 cm, there were some beads on the fibers. As the distance increased, beads disappeared, and diameter decreased. The diameter changed from 1.211 μm to 1.009 μm when the distance was from 10 cm to 25 cm [Figure 7(f)]. This was because that long distance could provide enough time for stretching the solution into fibers. However, beaded fibers came out again when the distance was more than 25 cm [Figure 7(d)]. This was due to the reduction of the field strength by increasing the distance from the needle to the target.<sup>24</sup> In general, a certain amount of voltage can provide a certain amount of field strength for stretching the polymer solution in a certain amount of distance. When the distance increased, the field strength for stretching the polymer solution needed to increase.

In contrast, if field strength was fixed and the operated distance exceeded the permitted one, the field strength was relatively weak to work. When the distance was too long [Figure 7(e)], the field strength was too weak to stretch the solution sufficiently. Therefore, drops and the fibers with insufficient stretch were sprayed onto the collector, leading to diameter of the fibers increased, and uniformity of the fibers decreased. It can be concluded that fibers with small diameter could be obtained via increasing collector distance, but when the distance was out of field strength's control, undesirable results would be produced.

**Concentration.** The effect of concentration on fiber morphology was significant. Too low concentration would make the solution reach the collection plate before full evaporation of the solvent.<sup>22</sup> In result, beads were generated, just as it was shown in Figure 8(a), when the concentration of the solution was 24 wt %. However, at a higher concentration, fewer beads can be observed [Figure 8(b)]. The changing of the fiber morphology can be attributed to the suppression of electrostatic and viscoelastic force to surface tension.<sup>25</sup> Surface tension tended to

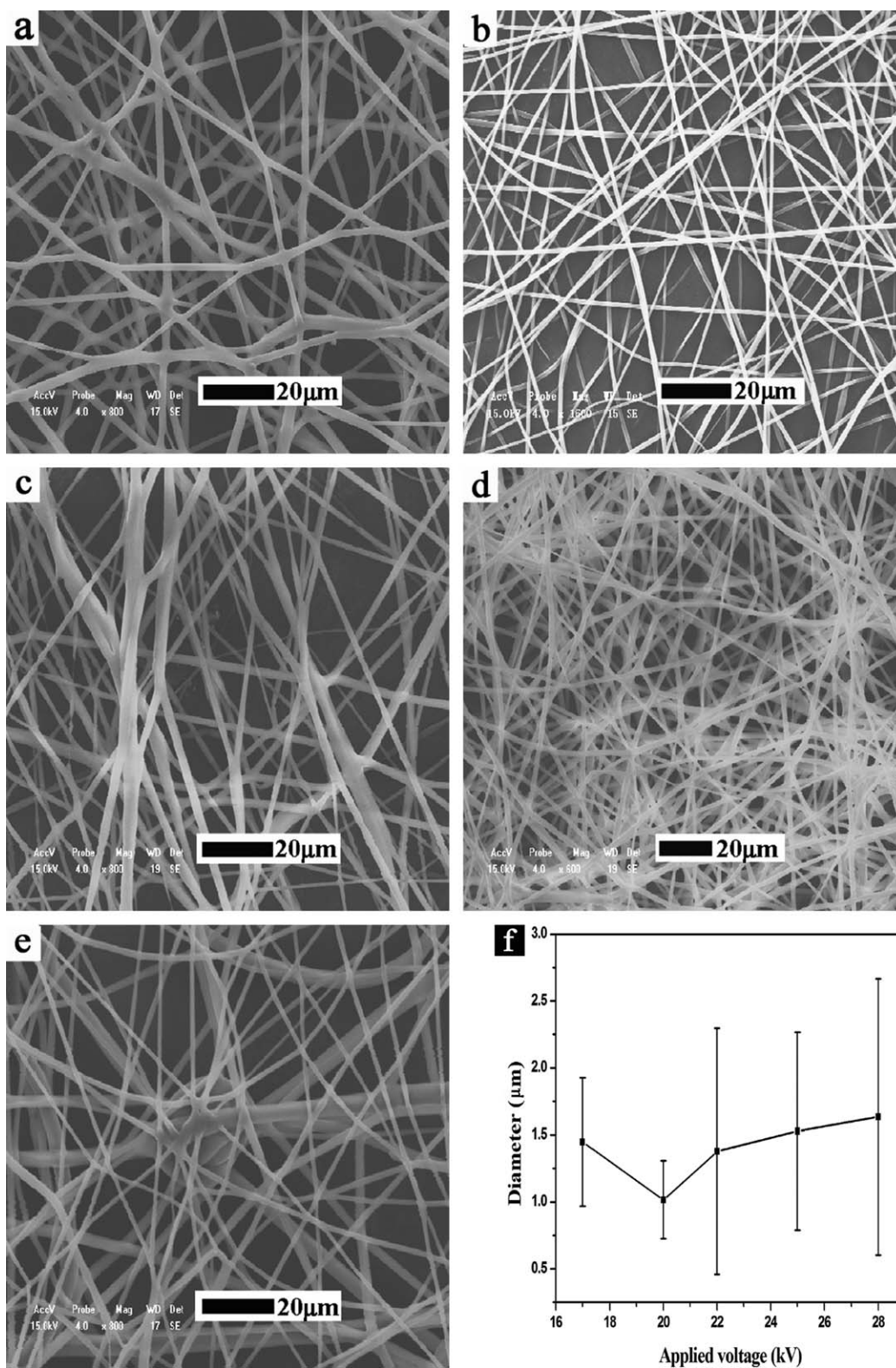


**Figure 6.** SEM images of PCL fibers, the voltages are (a) 17 kV, (b) 20 kV, (c) 22 kV, (d) 25 kV, (e) 28 kV; (f) is the diameter statistic result of the above images. (Beaded fibers are not included.)

minimize the surface area, and so it tried hard to convert the liquid jet into spherical drops; electrostatic force tended to increase the surface area, and thus it favored to format jets

rather than drops; the viscoelastic force resisted rapid changes in shape and tended to format fibers with smooth surfaces. It has been found that when the viscoelastic forces had a greater

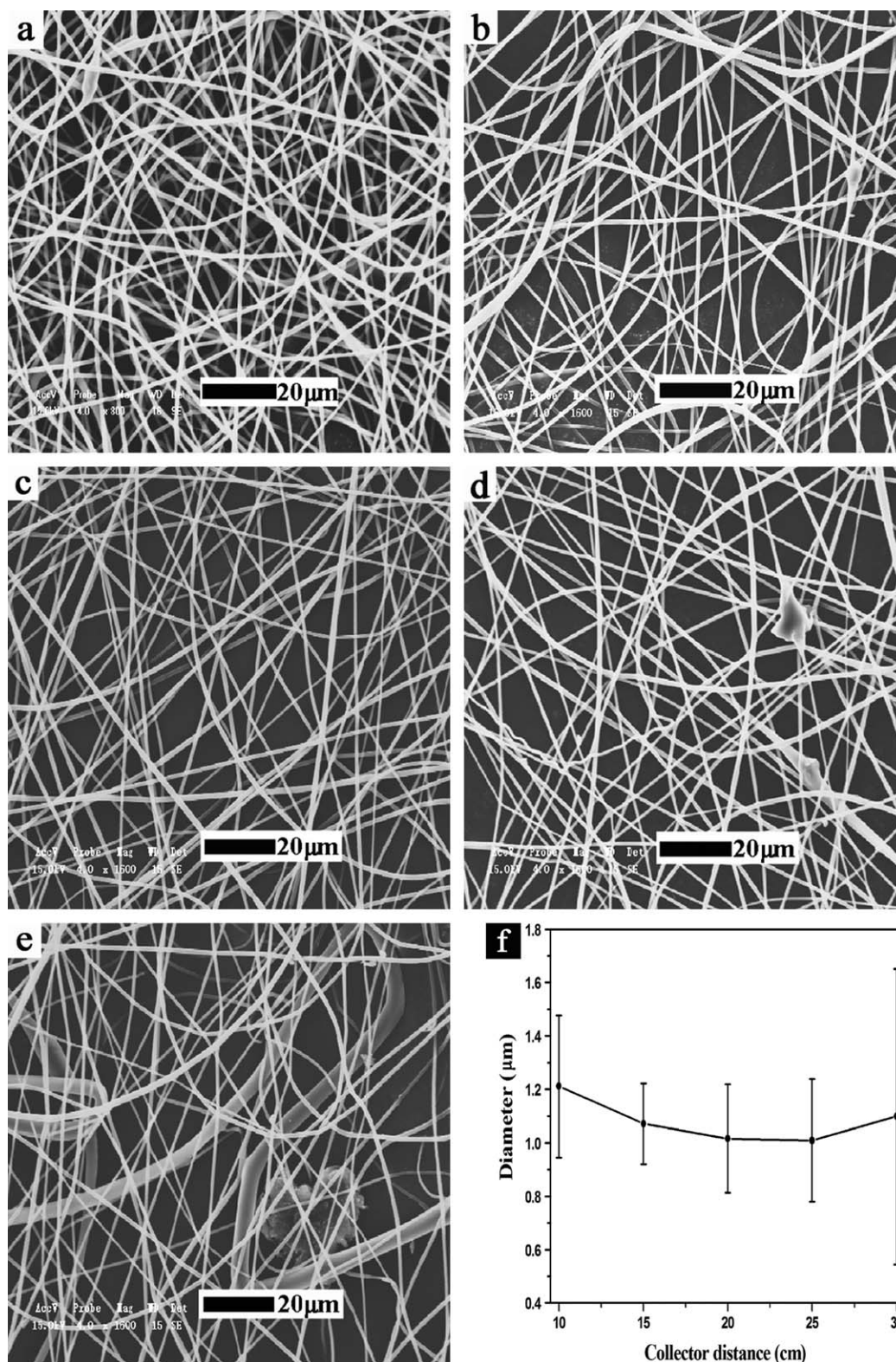


**Figure 7.** SEM images of PCLA fibers, the spinning distance are (a) 10 cm, (b) 15 cm, (c) 20 cm, (d) 25 cm, (e) 30 cm; (f) is the diameter statistic result of the above images. (Beaded fibers are not included.)

influence,<sup>20</sup> the fibers were smooth and uniform [Figure 8(c)]. When the concentration further increased to 30 and 32 wt %, drops can be seen clearly [Figure 8(d,e)]. This was because that

fiber formation was impeded by the high viscosity of the solution at high concentration. Besides, the uniformity was decreased with the increase of concentration [Figure 8(f)]. In

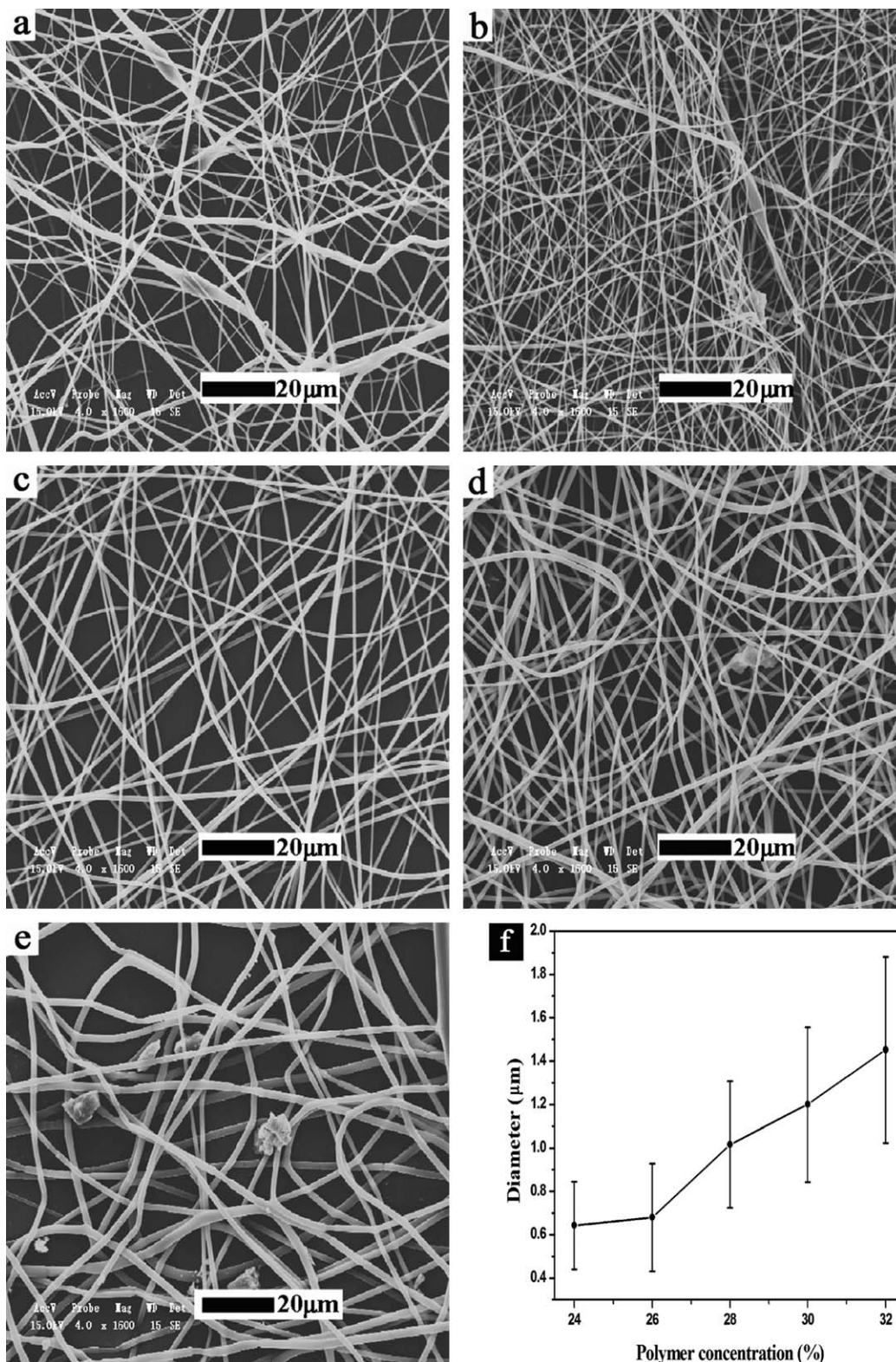


**Figure 8.** SEM images of PCL fibers, the concentrations of solution are (a) 24 wt %, (b) 26 wt %, (c) 28 wt %, (d) 30 wt %, (e) 32 wt %; (f) is the diameter statistic result of the above images. (Beaded fibers are not included.)

general, concentration is proportional to viscosity. Higher viscosity made the evaporation of solvent rapid, and then made the extension of jet more difficult. Therefore, thicker and non-

uniform fibers were formed. In summary, it seemed that low concentration was beneficial for obtaining slim and uniform fibers.

## CONCLUSIONS

PCLA copolymers with (ABA)<sub>n</sub> type was prepared via a mild method using hexamethylene diisocyanate (HDI) as chain extender. FT-IR, <sup>1</sup>H-NMR, and GPC data demonstrated that PLA and PCL-diOH had polymerized successfully. An experimental investigation of the optimum electrospinning conditions to produce PCLA micro-nanofibers was carried out. The results showed that when the ratio of DCM to DMF was 5/5, the voltage was 18 kV, the collecting distance was 20 cm and the concentration was 28 wt %, PCLA fibers with smoothest morphology and smallest diameter can be obtained. The effects of the four variables on fiber morphology, diameter, and uniformity were significant. As mixed solvent, ratio of DCM/DMF was found to be the most important factor on fiber diameter. On one hand, diameter decreased with the increase of DMF. On the other hand, uniformity was proportional to the content of DMF. Applied voltage was the second factor. Both exceeded low and high voltage could lead to sticky fibers, which further influenced the uniformity of fibers seriously. The third important factor was distance. Increase of the distance resulted in the reduction of fiber diameter and uniformity. Polymer concentration was the fourth factor. It seemed that low concentration was inclined to get fibers with small diameter. In general, process parameter was a key point for fabricating perfect fibers. The research on the influential factors can lay the foundation for further study. Besides, range analysis was an effective method that also suitable for other polymers.

## REFERENCES

1. Beachley, V.; Wen, X. *Mater. Sci. Eng. C: Mater.* **2009**, *29*, 663.
2. Li, D.; Wang, Y. L.; Xia, Y. N. *Adv. Mater.* **2004**, *16*, 361.
3. Son, W. K.; Youk, J. H.; Lee, T. S.; Park, W. H. *Polymer* **2004**, *45*, 2959.
4. Dotti, F.; Varesano, A.; Montarsolo, A.; Aluigi, A.; Tonin, C.; Mazzuchetti, G. *J. Ind. Text.* **2007**, *37*, 151.
5. Chen, J. P.; Chang, G. Y.; Chen, J. K. *Colloid Surface A* **2008**, *313–314*, 183.
6. Li, W. J.; Laurencin, C. T.; Caterson, E. J.; Tuan, R. S.; Ko, F. K. *J. Biomed. Mater. Res. A* **2002**, *60*, 613.
7. Wang, W.; Huang, H.; Li, Z.; Zhang, H.; Wang, Y.; Zheng, W.; Wang, C. *J. Am. Ceram. Soc.* **2008**, *91*, 3817.
8. Liu, M.; Cheng, Z.; Yan, J.; Qiang, L.; Ru, X.; Liu, F.; Ding, D.; Li, J. *J. Appl. Polym. Sci.* **2013**, *128*, 1095.
9. Ma, M.; Mao, Y.; Gupta, M.; Gleason, K. K.; Rutledge, G. C. *Macromolecules* **2005**, *38*, 9742.
10. Shin, H. J.; Lee, C. H.; Cho, I. H.; Kim, Y.; Lee, Y.; Kim, I. A.; Park, K.; Yui, N.; Shin, J. *J. Biomater. Sci. Polym. E* **2006**, *17*, 103.
11. Xie, J.; Li, X.; Xia, Y. *Macromol. Rapid. Commun.* **2008**, *29*, 1775.
12. Xua, C. Y.; Inai, R.; Kotaki, M.; Ramakrishna, S. *Biomaterials* **2004**, *25*, 877.
13. Mo, X. M.; Xu, C. Y.; Kotaki, M.; Ramakrishna, S. *Biomaterials* **2004**, *25*, 1883.
14. He, W.; Ma, Z. W.; Yong, T.; Teo, W. E.; Ramakrishna, S. *Biomaterials* **2005**, *26*, 7606.
15. Tsuji, H.; Mizuno, A.; Ikada, Y. *J. Appl. Polym. Sci.* **2000**, *76*, 947.
16. Varma, I. K.; Albertsson, A. C.; Rajkhowa, R.; Srivastava, R. K. *Prog. Polym. Sci.* **2005**, *30*, 949.
17. Zhang, J.; Xu, J.; Wang, H.; Jin, W.; Li, J. *Mater. Sci. Eng. C: Mater.* **2009**, *29*, 889.
18. Teng, C.; Yang, K.; Ji, P.; Yu, M. *J. Polym. Sci. Part A: Polym. Chem.* **2004**, *42*, 5045.
19. Ma, Z.; Kotaki, M.; Inai, R.; Ramakrishna, S. *Tissue Eng.* **2005**, *11*, 101.
20. Gu, S. Y.; Ren, J.; Vancso, G. J. *Eur. Polym. J.* **2005**, *41*, 2559.
21. Uyar, T.; Besenbacher, F. *Polymer* **2008**, *49*, 5336.
22. Bazbouz, M. B.; Stylios, G. K. *J. Appl. Polym. Sci.* **2008**, *107*, 3023.
23. Demir, M. M.; Yilgor, I.; Yilgor, E.; Erman, B. *Polymer* **2002**, *43*, 3303.
24. Yang, Y.; Jia, Z.; Li, Q.; Guan, Z. *IEEE T. Dielect. El. In.* **2006**, *13*, 580.
25. Li, D.; Xia, Y. *Adv. Mater.* **2004**, *16*, 1151.